Hydrogen Adsorption Storage on Single-Walled Carbon Nanotube Arrays by a Combination of Classical Potential and Density Functional Theory

Xianren Zhang,[†] Dapeng Cao,*[,†,‡] and Jianfeng Chen[†]

College of Chemical Engineering, Beijing University of Chemical Technology, Beijing 100029, China, Nanomaterials Technology Pte Ltd, 26 Ayer Rajah Crescent #07-02, Singapore 139944, Singapore

Received: January 16, 2003; In Final Form: March 28, 2003

The adsorptions of hydrogen both on square-packed single-walled carbon nanotube (SWCNT) arrays and on isolated nanotubes were investigated by a combination of a classical potential and density functional theory (DFT) method. Excess adsorption of hydrogen on the SWCNT with diameters of 1.225, 2.04, and 2.719 nm at 77 K and at ambient temperature, $T = 300$ K, has been calculated. DFT calculations indicate that the excess gravimetric storage capacity of exohedral adsorption of hydrogen on SWCNT array is as much as 30% of that of endohedral adsorption when the van der Walls (VDW) gap was fixed at 0.335 nm, while excess adsorption of hydrogen outside the nanotubes is close to or exceeds the excess endohedral adsorption for isolated nanotubes. The total excess gravimetric storage capacity (including endohedral and exohedral adsorptions) of hydrogen on open nanotube arrays of 2.719 nm is 7.1 wt % at 77 K and 4 MPa, while the total excess adsorption of hydrogen on open isolated nanotubes of 2.719 nm reaches 9.5 wt % at the same temperature and pressure. The two results both reach the gravimetric density of Department of Energy (DOE) target, 6.5 wt %, which means that the adsorption storage of hydrogen on SWCNTs has a practical significance. However, the total excess adsorption of hydrogen both on carbon nanotube arrays and on isolated nanotubes at 300 K does not exceed 1 wt % in the range of pressures that we studied and almost linearly increases with the increase of pressure. This is because the hydrogen molecules have enough kinetic energy to overcome the adsorption potential of SWCNTs at $T = 300$ K. For carbon nanotube arrays, the effect of VDW gap on hydrogen adsorption was investigated. Results indicate that in the range from 0.335 to 2.0 nm a larger VDW gap implies a greater excess gravimetric capacity and a smaller volumetric storage capacity, simultaneously. In addition, we also note that the choice of method used to determine the bulk density is key because it significantly affects the excess adsorption of hydrogen. In this work, DFT method is used to determine both the gas density in the confined space and the density in the bulk states simultaneously. It is more accurate than MBWR equation of state in solving the bulk density. In short, the predicted results of hydrogen storage capacities in SWCNTs at $T = 300$ and 77 K in this work are in reasonable agreement with experimentally measured data.

1. Introduction

A safe, effective, and cheap storage system is crucial for the future utilization of hydrogen as a pollution-free energy carrier. In recent years, the storage of hydrogen has attracted much attention owing to the availability of novel carbon nanomaterials, such as fullerenes, nanotubes, and nanofibers. Because the cylindrical structure of single-walled carbon nanotubes (SWCNTs) increases the adsorption potential in the tube and enhances storage capability, SWCNTs are an excellent candidate for H_2 storage.

Since Iijima[1] reported the synthesis of carbon nanotube in 1991, there have been many published experimental,[1−15] computer simulation,[16−29] and theoretical[30−34] studies of hydrogen adsorption on SWCNTs. Extensive experimental and theoretical works have recently been reviewed by Dresselhaus et al.,[35] Cheng et al.,[36] Simonyan and Johnson,[37] and Darkrim et al.[38] Because details are available in these references, we do not intend to discuss these works further here. To our knowledge, only four of all reported simulation work can reach the adsorption standards needed for practical process, which are the gravimetric storage capacity of 6.5 wt % or the volumetric storage capacity of 62 kg m^{-3}, issued by the Department of Energy (DOE, U.S.A.). They are Darkrim and Levesque,[26] Yin et al.,[27] Williams and Eklund,[29] and Lee and Lee.[34] Darkrim and Levesque[26] computed the adsorption properties of SWCNTs assuming SWCNTs in two arrangements (square and triangular lattices) constituted by 16 parallel tubes. They found by molecular simulations that at 77 K and 10 MPa, when the distances between carbon nanotubes increase to 1.1 nm, the hydrogen adsorption amount obtained was up to 11.24 wt %. In these thermodynamic and adsorbent geometric conditions, the volumetric density reached 60 kg m^{-3}. However, in their work, they provided the total adsorption amount rather than the excess one. Yin et al.[27] found by molecular simulations that adsorption of hydrogen in triangular array of open and closed carbon nanotubes with various diameters in a wide range of intertube distances exceeds the DOE gravimetric target. At 77 K, a capacity of 33 wt % is obtained for the arrays of narrow, open, or closed SWCNTs that are widely spaced, and volumetric capacities close to the DOE target are found for a range of interstitial spacings. Williams and Eklund[29] reported the results of molecular simulations of the physisorption of H_2 in finite-

* To whom correspondence should be addressed. E-mail: cao_dp@hotmail.com.
[†] Beijing University of Chemical Technology.
[‡] Nanomaterials Technology Pte Ltd.

10.1021/jp034110e CCC: $25.00
Published on Web 04/26/2003

diameter "ropes" of parallel single-walled carbon nanotube (SWCNT). They found delamination of nanotube ropes increased the gravimetric storage capacity. Compared with the three works mentioned above, Lee and Lee,[34] using electronic density functional theory and tight binding formalism, reported a surprising result, that (10,10) nanotubes could hold up to 14 wt % hydrogen at room temperature. In their research, the chemisorption and the interaction between atoms were considered. It was a significant difference from the physisorption of hydrogen mentioned above. Therefore, Simonyan and Johnson[37] commented that Lee's study is unfortunately somewhat misleading and their estimate of 14% is not realistic because the binding energies of the H_2 molecules are reduced by about 2 eV per molecule, indicating that the corresponding bulk pressure would have to be extraordinarily high, probably in the gigapascal range.

The density functional theory (DFT) method is a good theoretical approach to investigate the adsorption within slit and cylindrical pores in particular because the potential functions of the walls are well defined and analytically described. Gordon and Saeger[39] were the first ones using classic DFT method to study the hydrogen adsorption in SWCNTs. However, they only considered the adsorption of hydrogen inside the nanotube (endohedral adsorption) at the range of temperatures (150−315 K) for pores ranging from 0.8 to 2 nm without considering the adsorption of hydrogen on the external surface of the nanotubes or the adsorption of hydrogen in the interstices of SWCNT arrays. Not surprisingly, the computed gravimetric density falls short of the target of 6.5 wt %. In our previous work,[40] DFT method was used to investigate the hydrogen adsorption both inside the carbon nanotube and in the interstices of SWCNTs. It was found that when diameters of nanotubes reach 2.719 nm and SWCNTs are arranged in square lattices, which provide larger volume to host hydrogen molecules, rather than triangular arrangements, the excess gravimetric hydrogen storage can reach 13.2 wt % at 77 K and 6 Mpa, which is about 2 times that of the U.S. DOE target, while the volumetric capacity is less but near to the equivalent volumetric density of the U.S. DOE target. In our previous work, however, we did not optimize the adsorption process by changing the distances of two nearest carbon nanotubes (van der Waals gaps, VDW gaps).

Because the method used to determine bulk density affects excess adsorption significantly, here we recalculated the excess adsorption of hydrogen in the SWCNT array reported in our previous work by recomputing the bulk density with DFT method, rather than with the MBWR equation of state[41] used in our previous work. As an extension of our previous work, we studied the effects of VDW gaps on excess adsorption. Carbon nanotubes in SWCNTs are often found to be in tangled or partly aligned bundles. Some of them may not be ordered into arrays and are even isolated from others, so it is important to predict their adsorption storage capacities of hydrogen and compare them with those in ideal SWCNT arrays.

Accordingly, this paper was organized as follows. First, we briefly introduce classical potential model and the DFT method. Using the DFT method, we calculate the hydrogen adsorption in square arrays of SWCNTs with different diameters and separations and also calculate the hydrogen adsorption in isolated carbon nanotubes of different diameters. In the investigation, hydrogen adsorption in SWCNTs is calculated by splitting it into two parts of inside and outside tubes for a single isolated nanotube and in the SWCNT arrays by splitting it into two parts of inside nanotube and in interstices. Finally, we investigated the total adsorption of hydrogen on an isolated nanoube (including both endohedral and exohedral adsorption) and the total adsorption of hydrogen in the SWCNT arrays (including both endohedral and interstice adsorption).

TABLE 1: Parameters of Potential Models for Hydrogen and SWCNT

H_2		SWCNT		
σ_{ff} (nm)	ϵ_{ff}/k (K)	σ_{ss} (nm)	ϵ_{ss}/k (K)	ρ_{surf} (atoms/nm^2)
0.296	34.2	0.34	28.0	38.2

[a] ϵ = energy parameter; k = Boltzmann constant; subscripts ff and ss denote fluid and solid, respectively. [b] σ = molecular diameter; subscripts ff and ss denote fluid and solid, respectively.

2. Potential Models and Density Functional Theory

2.1. Potential Models. In this work, as many authors, we use the Lennard-Jones (LJ) potential to represent the interaction between a pair of hydrogen molecules,[21,28,29]

$$U_{LJ}(r) = 4\epsilon\left[\left(\frac{\sigma}{r}\right)^{12} - \left(\frac{\sigma}{r}\right)^{6}\right] \quad (1)$$

where r is the interparticle distance, ϵ is the well depth, and σ is the distance between a pair of molecules when the potential is zero.

The interaction between the wall and a hydrogen molecule inside a tube of SWCNTs, $\upsilon(r,R)$, is represented by the potential function proposed by Tjatjopoulos et al.[42]

$$\upsilon(r,R) = \pi^2\epsilon_{sf}\rho_{surf}\sigma_{sf}^{\ 2} \times \left[\frac{63}{32}\left[\frac{r}{\sigma}\left(2-\frac{r}{R}\right)\right]^{-10} F\left[-{}^9/_2,-{}^9/_2;1;\left(1-\frac{r}{R}\right)^2\right] - 3\left[\frac{r}{\sigma}\left(2-\frac{r}{R}\right)\right]^{-4} F\left[-{}^3/_2,-{}^3/_2;1;\left(1-\frac{r}{R}\right)^2\right]\right] \quad (2)$$

where $F[\alpha,\beta;\gamma;\chi]$ is the hypergeometric series, R is the radius of a tube, r is the distance from the wall, ρ_{surf}[39] is the density of carbon atoms on the wall, and the parameters ϵ_{sf} and σ_{sf} for solid−fluid interactions are obtained by the Lorentz−Berthelot combining rules. Equation 2 is obtained by integration of LJ potential over a cylindrical surface. The parameters used above are listed in Table 1.

Similar to eq 2, when adsorption takes place outside a single and isolated nanotube, the adsorbate−adsorbent interaction potential is obtained by integration of the LJ potential over the outer surface of nanotube[39] and is expressed as

$$\upsilon_{out}(r,R) = \pi^2\epsilon_{sf}\rho_{surf}R\sigma_{sf}^{\ 2}r^{-1} \times \left[\frac{63}{32}\left[\frac{r^2-R^2}{\sigma r}\right]^{-10} F\left[-{}^9/_2,-{}^9/_2;1;\left(1-\frac{r}{R}\right)^2\right] - 3\left[\frac{r^2-R^2}{\sigma r}\right]^{-4} F\left[-{}^3/_2,-{}^3/_2;1;\left(1-\frac{r}{R}\right)^2\right]\right] \quad (3)$$

We assume an idealized arrangement of carbon nanotubes to estimate the density of the adsorbent in SWCNT arrays. Figure 1 shows two configurations often used in computer simulations. The arrangement of square lattice was used in the work. The potential of a molecule in the interstice is approximated as a sum of interactions given by every nanotube forming the interstitial pore.

2.2. Density Functional Theory. For a system in an external field, $\upsilon(\mathbf{r})$, where $\mathbf{r}$ is the local position vector within the pore space, at a fixed temperature T and the chemical potential μ, the grand potential functional $\Omega[\rho(\mathrm{r})]$ is written as

$$\Omega[\rho(\mathbf{r})] = F[\rho(\mathbf{r})] + \int \mathrm{d}r\,[\upsilon(\mathbf{r}) - \mu]\rho(\mathbf{r}) \quad (4)$$

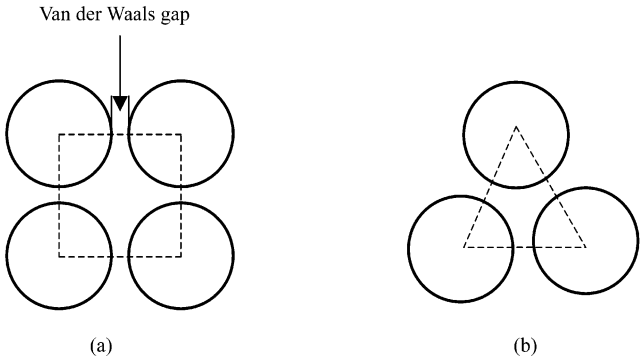

Figure 1. Cross section of two typical arrangements of the SWCNTs: (a) square array; (b) triangle array.

where $\rho(\mathbf{r})$ is the local density and $F[\rho(\mathbf{r})]$ is the intrinsic Helmholtz free-energy functional. The criterion for equilibrium is that the grand potential is a minimum, namely, the density profile $\rho(\mathbf{r})$ of the adsorbate within the pore satisfies the condition

$$\frac{d\Omega[\rho(\mathbf{r})]}{d[\rho(\mathbf{r})]} = 0 \tag{5}$$

The free-energy description employed in our calculation is the one proposed by Tarazona and co-workers,[43,44] in which the free energy of a fluid is split into repulsive and attractive contributions using the Weeks−Chandler−Anderson (WCA) perturbation scheme. Thus, we obtain

$$F[\rho(r)] = F_h[\rho(r)] + \frac{1}{2}\int\int d\mathbf{r}\, d\mathbf{r}'\, \rho(\mathbf{r})\rho(\mathbf{r}')\Phi_{attr}(|\mathbf{r}-\mathbf{r}'|) \tag{6}$$

where F_h is the hard-sphere Helmholtz free-energy functional and in the second term on the right-hand side the mean field approximation is used. The attractive part of the fluid−fluid potential, $\Phi_{attr}(|\mathbf{r}-\mathbf{r}'|)$, is represented by the WCA formulation[45] for the LJ potential

$$\Phi_{attr}(|\mathbf{r}-\mathbf{r}'|) = \begin{cases} -\epsilon_{ff} - U_{LJ}(r_c) & |\mathbf{r}-\mathbf{r}'| < r_m \\ \Phi_{LJ}(|\mathbf{r}-\mathbf{r}'|) - U_{LJ}(r_c) & r_m < |\mathbf{r}-\mathbf{r}'| < r_c \\ 0 & |\mathbf{r}-\mathbf{r}'| > r_c \end{cases} \tag{7}$$

where $r_m = 2^{1/6}\sigma_{ff}$, σ_{ff} is the size parameter for the LJ fluid, and r_c is the cutoff radius ($r_c = 5\sigma_{ff}$). The hard-sphere term can be further split into an ideal gas component and an excess component:

$$F_h[\rho(\mathbf{r})] = \int d\mathbf{r}\, \rho(\mathbf{r})[kT(\ln(\rho(\mathbf{r})) - 1) + f_{ex}(\bar{\rho}(\mathbf{r}))] \tag{8}$$

The excess Helmholtz free-energy per particle, f_{ex}, can be described by the Carnahan−Starling equation of state for a system of hard spheres[46] using a smoothed density, $\bar{\rho}$,

$$f_{ex}(\bar{\rho}(r)) = kT\eta\frac{(4-3\eta)}{(1-\eta)^2} \tag{9}$$

where $\eta = (\pi/6)\bar{\rho}d^3$ and the effective diameter d of a hard sphere is calculated as a function of temperature

$$\frac{d}{\sigma_{ff}} = \frac{\eta_1 kT/\epsilon_{ff} + \eta_2}{\eta_3 kT/\epsilon_{ff} + \eta_4} \tag{10}$$

where the parameters η_i can be referred to in the literature.[47] The smoothed density, $\bar{\rho}(\mathbf{r})$, is defined as

$$\bar{\rho}(\mathbf{r}) = \int w(|\mathbf{r}-\mathbf{r}'|;\bar{\rho}(\mathbf{r}))\rho(\mathbf{r}')\, d\mathbf{r} \tag{11}$$

where w is the weighted function given by

$$w(r;\rho) = w_0(r) + w_1(r)\rho + w_2(r)\rho^2 \tag{12}$$

where coefficients w_1, w_2, and w_3 are recommended by Tarazona et al.[44] As a result, from eqs 6−12, we know all of the expressions in eq 4. Substituting eq 4 into eq 5, consequently, we can solve eq 5 by iterations. Finally, the density profiles can be obtained.

The following commonly used variables are calculated:

Volumetric Storage Capacity (Vsc)

$$\mathrm{Vsc} = \frac{m_{H_2} - m^0_{H_2}}{V} \tag{13}$$

Gravimetric Storage Capacity (Gsc)

$$\mathrm{Gsc} = \frac{m_{H_2}}{m_{H_2} + m_{SWCNTs}} \tag{14}$$

Excess Adsorption (Ea)

$$\mathrm{Ea} = \frac{m_{H_2} - m^0_{H_2}}{m_{H_2} - m^0_{H_2} + m_{SWCNTs}} \tag{15}$$

where m_{H_2} is the total mass of hydrogen presented in the calculated volume, m_{SWCNTs} is the total mass of SWCNT, $m^0_{H_2}$ is the mass of hydrogen in bulk phase, and V is the effective volume. For example, the calculation of effective volume V of endohedral adsorption is based on the effective pore diameter, which has been defined as[48]

$$D_{eff} = D - \Delta \tag{16}$$

where D is the diameter measured between the centers of the first layer of solid atoms and Δ is the effective diameter of solid atoms treated as hard spheres. The effective diameter of solid atoms has been defined from the combining rule

$$\Delta = 2(\sigma_{sf} - 0.5\sigma_{ff}) \tag{17}$$

3. Results and Discussion

3.1. Adsorption of Hydrogen inside SWCNTs. We have calculated the adsorption isotherms of hydrogen inside SWCNTs with three different diameters, 1.225, 2.04, and 2.719 nm. DFT calculations are performed at 77 and 300 K over a pressure range from 0.2 to 20 MPa. Endohedral adsorption isotherms are shown in Figures 2 and 3, in which the adsorption amount was represented by reduced number density and excess gravimetric density of hydrogen molecule, respectively. One can see from Figure 2 that at $T = 300$ K the adsorption increases linearly with pressure for each pore size, and the smallest pore, 1.225 nm nanotube, gives the highest hydrogen density. Although increasing pore size will give a smaller reduced density, when pore size is greater than 2.04 nm, further increasing pore sizes do not give a significant uptake of hydrogen storage. In this particular case, the excess gravimetric storages are also given in Figure 3.

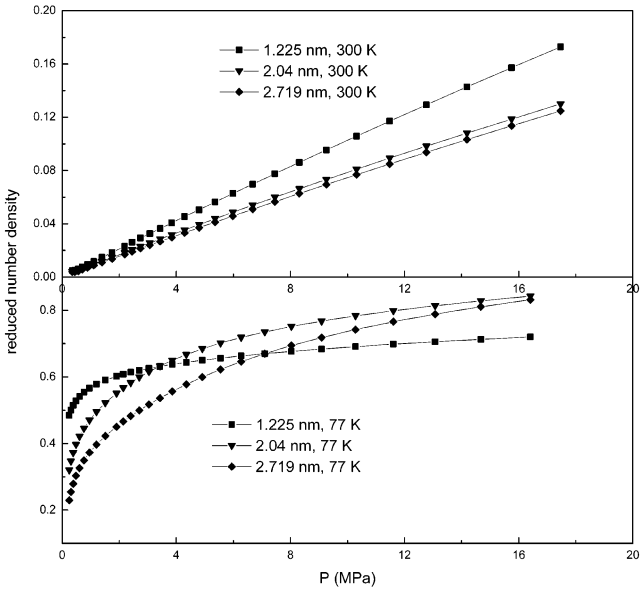

Figure 2. Adsorption isotherms of hydrogen in SWCNTs of different diameters at $T = 300$ and 77 K.

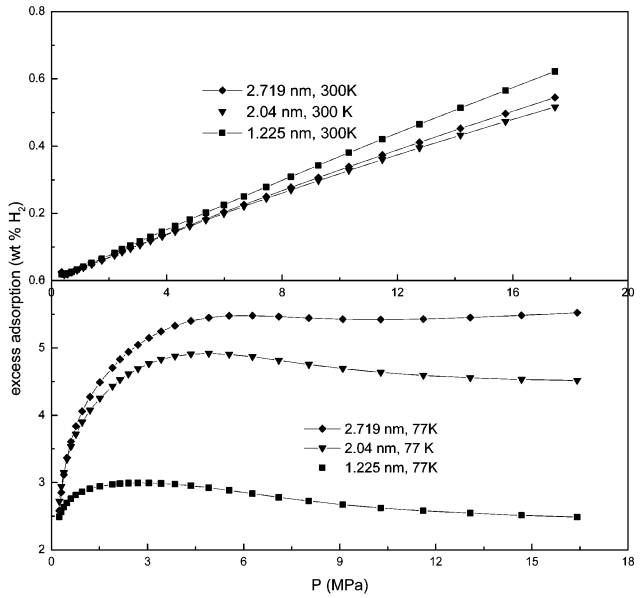

Figure 3. Excess gravimetric storage isotherms of hydrogen in the SWCNTs of different diameters at $T = 300$ and 77 K.

For adsorption at 77 K, it is clear that the optimum pore size for hydrogen storage depends on pressure. At pressures less than 3.5 MPa, the tube with a diameter of 1.225 nm holds more hydrogen molecules per volume. But at pressures greater than that, a larger pore will hold more. Different trends are shown in Figure 3 in which adsorption isotherms are expressed by excess gravimetric capacity. The excess gravimetric storage capacity of SWCNTs improves when the pore size increases. For example, the maximum of excess endohedral adsorption for 2.719 nm reaches close to the DOE target of 6.5 wt % at 77 K and a pressure range from 3 to 6 MPa. The fact that the larger pores are more effective in this case is because at 77 K the amount of adsorbed hydrogen increases rapidly, as $\sim D^2$, whereas the weight of carbon nanotube increases more slowly with the increase of nanotube diameter, as $\sim D$.

The potentials calculated from eqs 2 and 3 for the inside and outside of the nanotube, using established parameter values listed in Table 1, are shown in Figure 4. The potential inside a

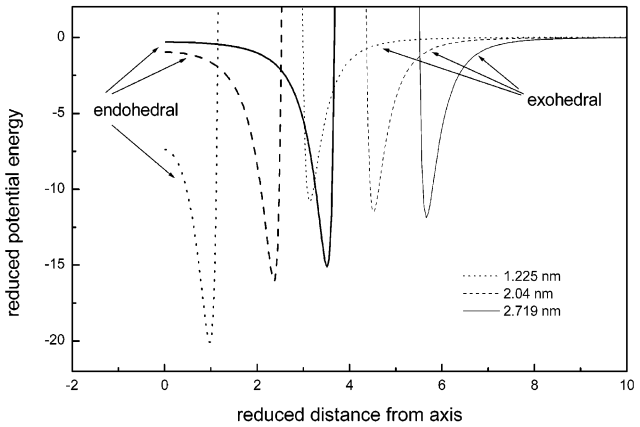

Figure 4. Fluid−wall interactions for hydrogen molecules inside and outside of the nanotubes.

nanotube strongly increases as tube diameter decreases, while the depth of the potential outside the nanotube decreases as the tube diameter decreases.

There are many factors that affect the amount of adsorption, of which two important ones are space and the attractive force. The space accessible to hydrogen molecules and the effective volume increase with the pore size, which can increase the amount of adsorption. On the other hand, the attractive force decreases with the increase of pore size, which causes the decrease of the amount of adsorption. However, at 300 K, the attractive force shows more important effects than the space effect in overcoming the furious thermal vibration, while at 77 K, the space accessible would significantly affect the amount of adsorption because at this temperature the pore is always filled by hydrogen molecules.

For the pores studied, the excess gravimetric capacities are not very sensitive to the pore size at 300 K and the adsorption of hydrogen inside the tubes is not much greater than those for compressed gas. However, when temperature decreases to 77 K, the pore size significantly affects the excess adsorption as shown in Figure 3. One can see that for different pore sizes the excess gravimetric capacities reach a maximum at different pressures. The maximum excess adsorption reaches 5.5 wt % for the tube of 2.719 nm at about 5 MPa, while for the tube of 1.225 nm, the maximum adsorption is only about 3 wt % at 3 MPa.

3.2. Adsorption of Hydrogen in the Interstices. The adsorption isotherms of hydrogen in interstices at 300 and 77 K, where the van der Waals distance is fixed at 0.335 nm, are shown in Figures 5 and 6. Adsorption amount in Figure 5 is expressed as reduced number density, while it is represented by excess gravimetric density in Figure 6. At $T = 300$ K, the reduced number density of hydrogen in three pores is almost the same in the low-pressure ranges. With the increase of pressure, the reduced density of hydrogen in the larger interstitial space is larger. It can be seen from Figure 6 that excess gravimetric density increases with increasing interstitial spaces at $T = 300$ K, as we expected.

At 77 K and very low pressure, the smaller interstices yield a somewhat greater number density but show smaller excess gravimetric storage capacities, while at high pressure, the situation is different, and the increased volumes of large interstices offer not only the increase of number densities but also the excess gravimetric densities. The peak values of excess gravimetric storage capacities are 1.2, 1.5, and 1.8 wt % for interstices corresponding to 1.225, 2.04, and 2.719 nm SWCNTs, respectively. The optimal pressures for the three pores are

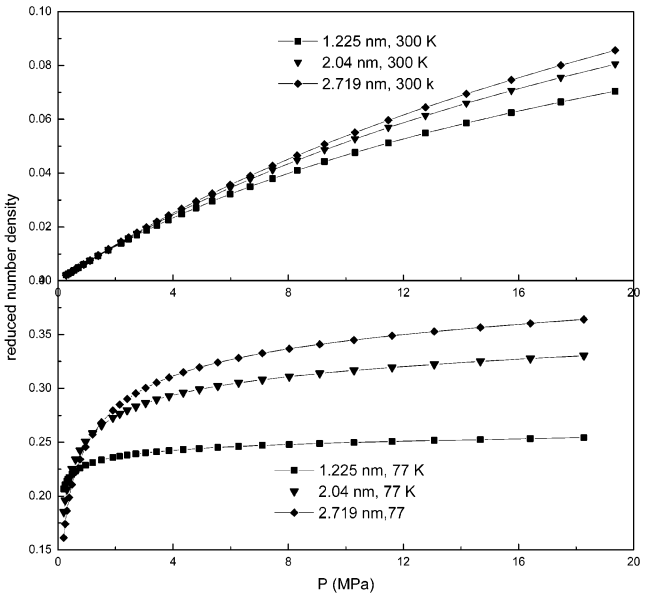

Figure 5. Adsorption isotherms of hydrogen in interstitial spaces of the SWCNT arrays with different pore diameters at $T = 300$ and 77 K.

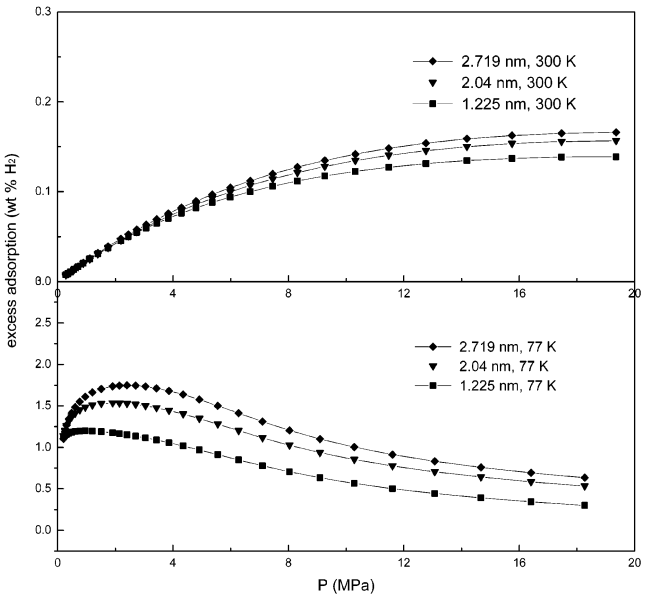

Figure 6. Excess gravimetric storage isotherms of hydrogen in the interstices of different SWCNT arrays at $T = 300$ and 77 K.

located at 0.9, 1.9, and 2.4 MPa, respectively. Note that for the smallest interstice of 1.225 nm SWCNTs, the excess gravimetric storage capacity becomes negative at very high pressure, 18 MPa. This is because in the small interstice, as shown in Figure 1, there is some void volume not to be accessible for adsorbate molecules, such as the corners where two nanotubes are near to each other. As pressure increases, the density is almost the same as that of compressed gas, so the existence of void volume makes the total amount of adsorption in interstice less than that of the compressed gas.

Figure 7 shows the volumetric storage capacities of SWCNTs with different pore size at $T = 300$ and 77 K as a function of pressure. One can see from Figure 7 that at $T = 300$ K for each diameter the volumetric storage capacities increase linearly with pressure and the smallest pore, 1.225 nm pore, gives the highest value at 18 MPa, 6 kg/m^3, far from the target volumetric storage capacity of 62 kg/m^3. Although increasing pore size will give a smaller volumetric storage capacity, when the pore size is

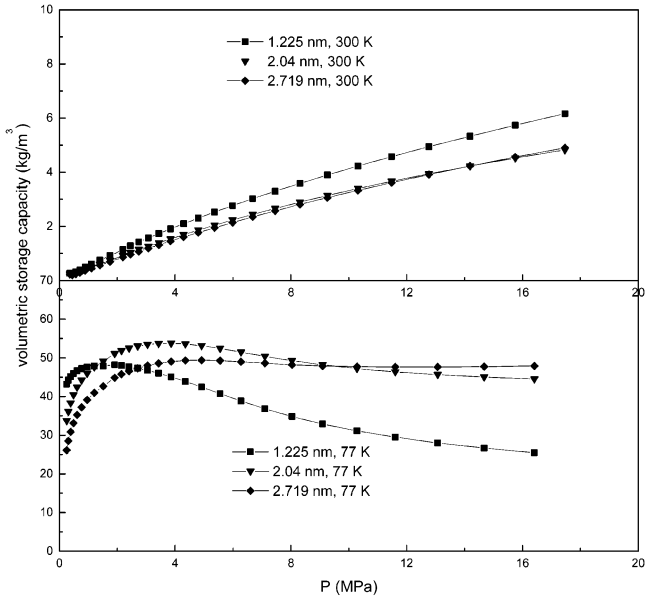

Figure 7. Volumetric storage capacities of hydrogen on the SWCNTs with different sizes at $T = 300$ and 77 K.

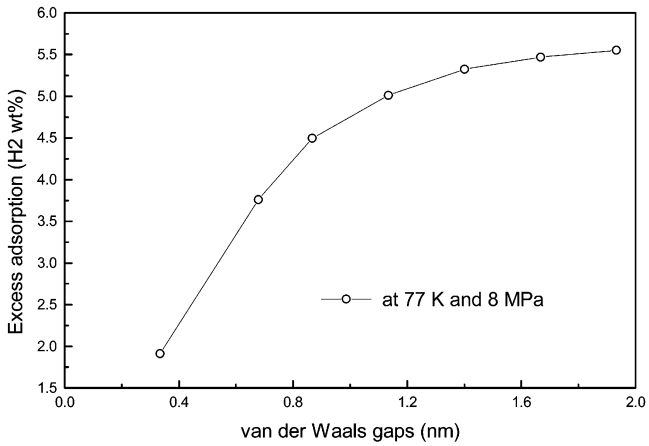

Figure 8. Excess gravimetric storage of hydrogen in the interstice of 2.719 nm SWCNT arrays with different VDW gaps at 77 K and 8 MPa.

greater than 2.04 nm, further increasing pore size does not give a significant change of volumetric storage capacity. The observation is the same for the gravimetric denisity of endohedral adsorption at $T = 300$ K. Figure 7 also shows the volumetric storage capacities of SWCNTs at 77 K, and there is a maximum for each pore size of SWCNTs. The peak values for the volumetric storage capacities are 48, 54, and 49 kg/m^3 at 2, 3.9, and 5 MPa for 1.225, 2.04, and 2.719 nm, respectively.

3.3. The Effects of van der Waals Gap on Hydrogen Adsorption. DFT calculations of the adsorption of hydrogen in the interstices of SWCNTs require much CPU time because the region of integral is in two dimensions rather than one as in the cylindrical pore. The CPU time for DFT calculation of hydrogen adsorption in the interstice is much more than that used in computer simulation. Hence DFT is not recommended to investigate the hydrogen adsorption in pores of complicated geometries, such as the case of adsorption of hydrogen in the interstices of SWCNTs. With the increase of VDW gaps, the computing times become very large, so we only investigate the effects of VDW gaps in the range of 0.335−2 nm.

Figures 8 and 9 show excess gravimetric and volumetric storage capacity of 2.719 nm SWCNTs as a function of VDW distances over 0.335−2 nm at $p = 8$ MPa and $T = 77$ K. The

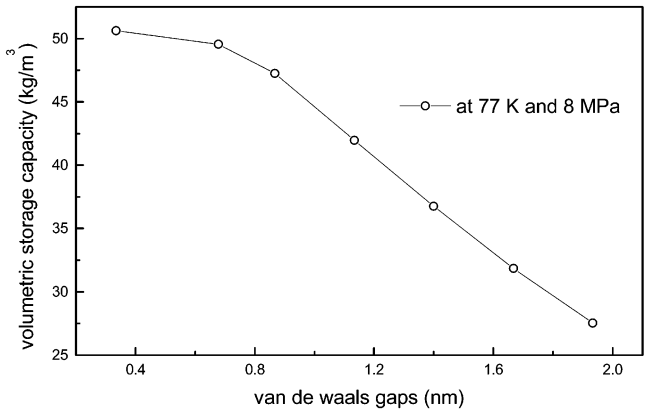

Figure 9. Volumetric storage capacities of hydrogen on 2.719 nm SWCNT arrays at $T = 77$ K and $p = 8$ MPa.

excess gravimetric density increases rapidly when VDW gap increases from 0.335 to 1.4 nm. On further increase of the VDW distance from 1.4 to 2.0 nm, the excess adsorption does not change significantly. This is because the attractive force from the nanotube decreases rapidly. Although a larger VDW gap gives more excess gravimetric capacity, the volumetric storage capacity reduces, as one can see from Figure 9. The explanation for this can be given as follows. The increase of VDW distance causes the increase of the volume to hold hydrogen molecules, at least the density greater than that of compressed gas, which can increase the amount of excess adsorption. On the other hand, the attractive force from the nanotube decreases with the increase of VDW gap, which makes the increase of adsorption slower than the increases of pore volume. The volumetric storage capacity decreases as a result.

3.4. Exohedral Adsorption of Hydrogen on a Single Isolated Nanotube. We have calculated hydrogen adsorption on the external surface of an isolated tube. For isolated tubes, it means that tubes are far enough apart from each other that the interaction between adsorbate molecule and other tubes in the array is negligible.

Although no one has studied the exohedral adsorption of hydrogen for an isolated SWCNT, Yin and co-workers[49] demonstrated that endohedral and exohedral adsorption of nitrogen can take place simultaneously. Simonyan et al.[50] thought that exohedral adsorption of xenon was about 10^{-6} times less than endohedral adsorption at 95 K and very low pressure.

For an isolated SWCNT, we also performed DFT calculation of the exohedral adsorption of hydrogen. Adsorption isotherms are shown in Figure 10, in which adsorption amount is represented by excess gravimetric storage capacity. Interestingly, the adsorption of hydrogen on external surface of SWCNT is not negligible compared with endohedral adsorption. Especially for the smaller pore, for example, the maximal adsorption amount of hydrogen on external surface is 5.3 wt %, greater than the 3.0 wt % inside SWCNT. However, it is important to note that the exohedral adsorption isotherms are qualitatively different from that for endohedral adsorption. A rapid decay for excess exohedral adsorption was observed as pressure increases from its optimal value. We think that the difference was caused by the difference of the interaction potentials between a hydrogen molecule with internal and external surfaces of an isolated nanotube, as shown in Figure 4.

From Figure 10, one can see that the excess gravimetric density decreases as pore size increases. This seems to conflict with the conclusion shown in Figure 4 that potential energy from external surface of the nanotube increases as pore size

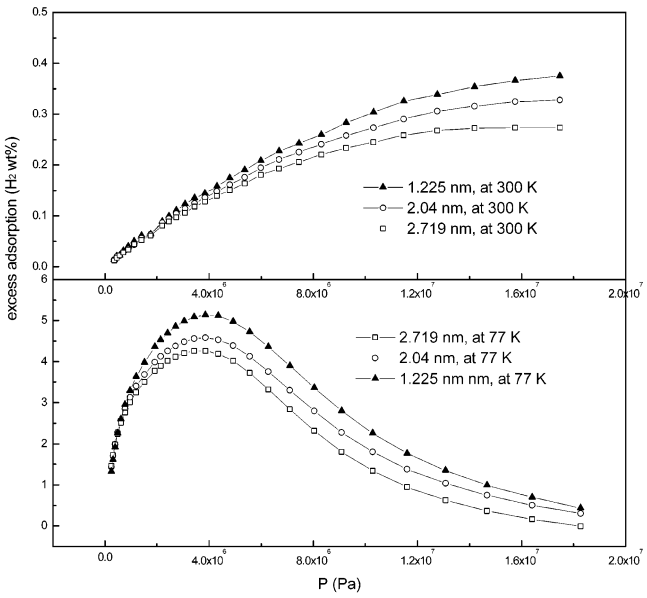

Figure 10. Excess gravimetric storage isotherms of hydrogen outside single isolated SWCNTs at $T = 300$ and 77 K.

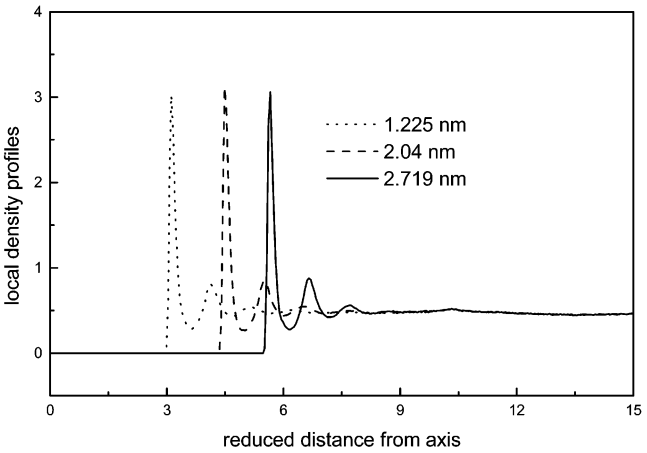

Figure 11. Local density profiles of hydrogen absorbed on the nanotube external surfaces of different diameters at $T = 77$ K.

increases. The local density profiles shown in Figure 11 provide a good answer to this question. The local densities of hydrogen on nanotube external surface of different diameters are almost the same, and no significant difference appears. This means that the difference of potential energy caused by different pore sizes has minor effects on adsorption. In addition, because the excess adsorption amount,

$$m_{H_2} - m^0_{H_2} = \int_{(D+\Delta')/2}^{\infty} (\rho(r) - \rho_{bulk}) 2\pi r \, dr$$

is directly proportional to $D + \Delta'$ (because local densities are the same for the three pore sizes and Δ' is approximately equal to σ_{sf}) and the mass of SWCNT is directly proportional to the diameter of nanotube D, the excess gravimetric density is directly related to $(D + \sigma_{sf})/D$, that is, $1 + \sigma_{sf}/D$. Therefore, the excess gravimetric density decreases as pore size increases.

3.5. Total Adsorption of Hydrogen on Isolated Nanotubes and on Nanotube Arrays. Adsorption isotherms of hydrogen in the interior of tube and the interstitial space were calculated from independent DFT runs. The total adsorption was obtained by simply adding the amounts adsorbed in the tube and interstice at each pressure.

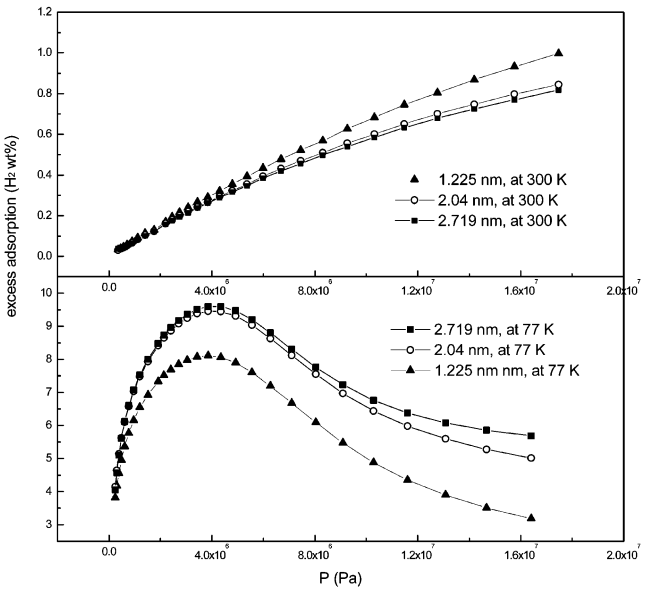

Figure 12. Total excess gravimetric storage isotherms of hydrogen on isolated nanotubes of different diameters at $T = 300$ and 77 K.

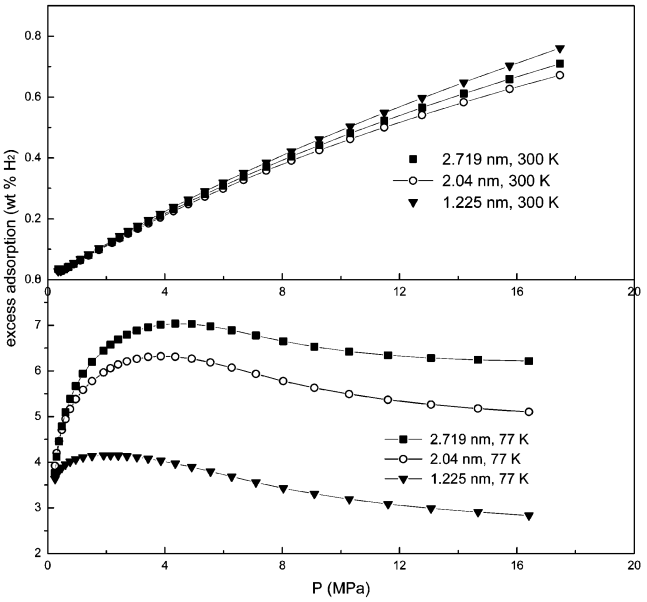

Figure 13. Total excess gravimetric storage isotherms of hydrogen on the carbon nanotube arrays of different diameters at $T = 300$ and 77 K.

Because some tubes in SWCNTs are isolated or tangled and some are found in partly aligned bundles, we consider the total adsorptions of isolated nanotubes and nanotube arrays, respectively. For isolated nanotubes, their ends can be either open or closed. If the tube ends are closed, only exohedral adsorption can take place; if they are open, both endohedral and exohedral adsorption occur simultaneously. For the tube arrays, if the tube ends are closed, only interstitial adsorption can take place; if they are open, both endohedral and interstitial adsorption also appear simultaneously.

The total excess adsorption isotherms of hydrogen on isolated nanotubes and on nanotube arrays are shown in Figures 12 and 13, respectively. Note that the hydrogen adsorptions on closed isolated nanotubes and on closed nanotube arrays have been given in Figures 5 and 10. Therefore, they are not shown in Figures 12 and 13.

For nanotube arrays arranged in square lattices, at $T = 77$ K, the total excess adsorptions have a maximum for each pore size of SWCNTs. The peak values for the excess gravimetric storage capacities are 4.2, 6.3, and 7.1 wt % at 4.2, 3.8, and 4 MPa for 1.225, 2.04, and 2.719 nm, respectively. At $T = 300$ K, the total excess adsorption increases with increasing pressure; however, its value does not exceed 1 wt % in the range of pressures studied. The observation is in good agreement with that from Tibbetts et al.[7] On the basis of experimental measure of the hydrogen adsorption in nine kinds of carbon materials, they thought that it was not likely for any carbon materials to reach a gravimetric density at ambient temperature greater than 1 wt %.

TABLE 2: Comparisons of Calculated Gravimetric Storage of Hydrogen on SWCNTs and Reported Experimental Results

material	source	max wt % H_2	T (K)	p (MPa)
2.719 nm, open, isolated	this work	9.6	77	4
2.719 nm, open, array	this work	7.1	77	4
SWCNT (DFT)	ref 39	1.2	150	10
SWCNTs (GCMC[a])	ref 23	2	80	10
SWCNTs (GCMC[a])	ref 26	11	80	10
SWCNTs (GCMC[a])	ref 29	9.5	77	10
SWCNTs (high purity)	ref 3	8.25	80	7.18
SWCNTs (50% pure)	ref 4	4.2	300	10.1
SWCNTs (high purity)	ref 7	0.05	300	3.59

[a] Grand canonical Monte Carlo method.

For open isolated SWCNT, at 77 K, the total excess adsorption shows a maximum at about 4 Mpa pressure. The optimum excess gravimetric storage capacities reach 8.1, 9.5, and 9.6 wt % for open isolated nanotubes corresponding to 1.225, 2.04, and 2.719 nm, respectively. Likewise, the total excess adsorption at 300 K increases with increasing pressure, and its value does not exceed 1 wt % in the range of pressures studied. Comparing the total excess adsorption on isolated carbon nanotubes and that on the nanotube arrays arranged in square lattices, we found that the isolated carbon nanotubes give higher excess gravimetric storage capacities. The findings coincide well with that from Williams and Eklund.[29]

For nanotubes arranged in square lattices, at 77 K, the total excess adsorption shows a maximum of 13.2 wt % for 2.719 nm SWCNTs in our previous work, different from 7.1 wt % in this work. The root of this significant deviation is from the different methods in calculating bulk density. In our previous DFT calculation of hydrogen adsorption in SWCNTs, MBWR equation of state is used to solve the bulk density, while DFT method is used here to determine both the gas density in the confined space and the density in the bulk states simultaneously. The results in this work were thus thought to be more reliable. For the adsorption of hydrogen outside an isolated nanotube, the method for determining bulk density becomes very critical because it has dramatic effects on excess adsorption. Therefore, we should pay considerable attention to the method for determining the bulk density because of its significant effect on the excess adsorption of hydrogen storage.

3.6. Comparison between DFT Calculations and Experimental Measurements. Comparisons between experimental and simulated gravimetric hydrogen capacities are complicated because experimental data of hydrogen storage capacities came from different purity nanotube samples without any ordered arrays. However, for a clear review, we show some relative results of hydrogen adsorption on SWCNTs in Table 2.

Ye et al.[3] reported hydrogen adsorption on purified SWCNT samples at 80 K over a pressure range from 0.5 to 160 bar. They found that the hydrogen adsorption can reach 8.25 wt % at $T = 80$ K and $p = 7.18$ Mpa (see Table 2), which is in good

agreement with our computed results of 8.3 wt % (2.719 nm isolated carbon nanotube, open) at $T = 77$ K and $p = 7.1$ MPa.

Tibbetts et al.[7] have recently studied adsorption of hydrogen on nine different carbon materials (including SWCNTs from Rice University) at pressures up to 11 MPa and temperatures from 193 to 773 K and found that only 0.05 wt % (see Table 2) excess amount for adsorption of hydrogen on SWCNTs at 300 K and 3.59 Mpa, was obtained. The adsorption calculated here at 300 K and 3.8 MPa is in the range from 0.02 wt % (2.04 nm SWCNT array, closed) to 0.3 wt % (1.225 nm isolated carbon nanotube, open). Obviously, the calculated results encompass the experimental data.

Note that Dillion et al.[2] and Liu et al.[4] reported much higher gravimetric storage capacities (see Table 2) of SWCNTs at ambient temperature than that predicted in this work. As pointed out by Simonyan and Johnson,[37] the existence of chemisorption may be an answer to the deviation.

4. Conclusions

At $T = 300$ K, the excess gravimetric capacities of endohedral adsorption are not very sensitive to the pore size and the adsorption inside tubes is not much greater than those for compressed gas. However, when temperature decreases to 77 K, the pore size significantly affects the excess adsorption of hydrogen, and for different pore size, the excess gravimetric capacities reach a maximum at different pressures. The maximum excess adsorption of hydrogen inside the 2.719 nm tube reaches 5.5 wt % at a storage pressure of about 5 MPa, while for 1.225 nm, the maximum excess amount is about 3 wt % at 3 MPa. DFT calculations indicate that the excess gravimetric storage capacities of exohedral adsorption of hydrogen on SWCNT arrays are as much as 30% of those of endohedral adsorption when the VDW gap was fixed at 0.335 nm. Therefore, exohedral adsorption should be taken into account in calculating total adsorption amount.

At $T = 77$ K, the total excess adsorption of hydrogen (including endohedral and exohedral adsorptions) shows a maximum for each pore size of SWCNTs arrays. The optimum excess gravimetric storage capacities are 4.2, 6.3, and 7.1 wt % at 4.2, 3.8, and 4 MPa for 1.225, 2.04, and 2.719 nm, respectively. Only SWCNT arrays of 2.719 nm can reach the gravimetric density of DOE targets, 6.5 wt %, even though the volumetric storage capacities are less than targets. We also investigated the effects of VDW gap on excess adsorption and found that in a range from 0.335 to 2.0 nm, as the VDW gap gets larger, the excess gravimetric capacity increases.

It is necessary to include the adsorption amount of hydrogen on the external surface of an isolated SWCNT in calculating total adsorption because excess adsorption outside nanotubes is close to or exceeds the excess endohedral adsorption. At $T = 77$ K, the total excess adsorption shows a maximum at about $p = 4$ MPa. These optimal excess gravimetric storage capacities are 8.1, 9.5, and 9.6 wt % for open isolated nanotubes corresponding to 1.225, 2.04, and 2.719 nm, respectively. Comparison of the total excess adsorptions on isolated carbon nanotubes and on the nanotube arrays arranged in square lattices indicates that the isolated carbon nanotubes give higher excess gravimetric storage capacities, but the volumetric storage capacities would inevitably become smaller.

At $T = 300$ K, the total excess adsorptions in isolated nanotubes and in the nanotube arrays of SWCNTs, increase with the increase of pressure and their value does not exceed 1 wt % in the range of the pressures studied.

Additionally, considerable attention should be paid to the method to determine the bulk density because it may significantly affect the excess adsorption of hydrogen storage. DFT method is used to determine both the gas density in the confined space and the density in the bulk states simultaneously in this work. This is more accurate than MBWR equation of state in solving the bulk density. The predicted hydrogen capacities in SWCNTs at ambient temperature and at 77 K are in reasonable agreement with experimentally measured capacities. In short, the DFT method is an effective approach to investigate the fluid confined in heterogenenous materials in which the interaction between solid walls and confined molecules can be expressed by a well-defined analytical potential.

Acknowledgment. This work was supported by the Key Research of Science & Technology of the Ministry of Education, China (Grant No. 0202), the State Key Fundamental Research Plan (Grant No. G2000048010), Natural Science Foundation (NSF) of China (Grant Nos. 20236010 and 20276004), and China Postdoctoral Science Foundation. The authors are grateful to Professor Wenchuan Wang for his helpful suggestions in preparation of this paper.

References and Notes

(1) Iijima, S. Helical microtubules of graphitic carbon. *Nature* **1991**, *354*, 56.

(2) Dillon, A. C.; Jones, K. M.; Bekkedahl, T. A.; Kiang, C. H.; Bethune, D. S.; Heben, M. J. Storage of hydrogen in single-walled carbon nanotubes. *Nature* **1997**, *386*, 377.

(3) Ye, Y.; Ahn, C. C.; Witham, C.; Fultz, B.; Liu, J.; Rinzler, A. G.; Colbert, D.; Smith, K. A. Smalley, R. E. Hydrogen adsorption and cohesive energy of single-walled carbon nanotubes. *Appl. Phys. Lett*. **1999**, *74* (16), 2307.

(4) Liu, C.; Fan, Y. Y.; Liu, M.; Cong, H. T.; Cheng, H. M.; Dresselhaus, M. S. Hydrogen storage in single-walled carbon nanotubes at room temperature. *Science* **1999**, *286*, 1127.

(5) Chen, P.; Wu, X.; Lin, J.; Tan, K. L. High H_2 uptake by alkali-doped carbon nanotubes under ambient pressure and moderate temperatures. *Science* **1999**, *285*, 91.

(6) Yang, R. T. Hydrogen storage by alkali-doped carbon naotubes-revisited. *Carbon* **2000**, *38*, 623.

(7) Tibbetts, G. G.; Meisner, G. P.; Olk, C. H. Hydrogen storage capacity of carbon nanotubes, filaments and vapor-grown fibers. *Carbon* **2001**, *39*, 2291.

(8) Shiraishi, M.; Takenobu, T.; Yamada, A.; Ata, M.; Kataura, H. Hydrogen storage in single walled carbon nanotube bundles and peapods. *Chem. Phys. Lett.* **2002**, *358*, 213.

(9) Gundiah, G.; Govindaraj, A.; Rajalakshmi, N.; Dhathathreyan, K. S.; Rao, C. N. Hydrogen storage in carbon nanotubes and related materials. *J. Mater. Chem*. **2003**, *13*, 209.

(10) Kajiura, H.; Tsutsui, S.; Kadono, K.; Ata, M.; Murakami, Y. Hydrogen storage capacity of commercially available carbon materials at room temperature. *Appl. Phys. Lett*. **2003**, *82*, 1105.

(11) Ci, L. J.; Zhu, H. W.; Wei, B. Q.; Xu, C. L.; Wu, D. H. Annealing amorphous carbon nanotubes for their application in hydrogen storage. *Appl. Surf. Sci*. **2003**, *205*, 39.

(12) Wang, Q. K.; Zhu, C. C.; Liu, W. H.; Wu, T. Hydrogen storage by carbon nanotube and their films under ambient pressure. *Int. J. Hydrogen Energy* **2002**, *27*, 497.

(13) Zhuttel, A.; Sudan, P.; Mauron, P.; Kiyobayashi, T.; Emmenegger, C.; Schlapbach, L. Hydrogen storage in carbon nanostructures. *Int. J. Hydrogen Energy* **2002**, *27*, 203.

(14) Zhu, H. W.; Cao, A. Y.; Li, X. S.; Xu, C. L.; Mao, Z. Q.; Ruan, D. B.; Liang, J.; Wu, D. H. Hydrogen adsorption in bundles of well aligned carbon nanotubes at room temperature. *Appl. Surf. Sci*. **2001**, *178*, 50.

(15) Skowronski, J. M.; Scharff, P.; Pfander, N.; Cui, S. Room-temperature electrochemical opening of carbon nanotube followed by hydrogen storage. *Adv. Mater*. **2003**, *15*, 55.

(16) Zhou, L. G.; Shi, S. Q. Molecular dynamic simulations on tensile mechanical properties of single walled carbon nanotubes with and without hydrogen storage. *Comput. Mater. Sci*. **2002**, *23*, 166.

(17) Gordillo, M. C.; Boronat, J.; Casulleras, J. Zero temperature equation of state of quasi-one-dimensional H2. *Phys. Rev. Lett*. **2000**, *85*, 2348.

(18) Gordillo, M. C.; Boronat, J.; Casulleras, J. Isotoptic effects of hydrogen adsorption in carbon nanotubes. *Phys. Rev. B* **2001**, *65*, 014503.

(19) Kostov, M. K.; Cheng, H.; Herman, R. M.; Cole, M. W.; Lewis, J. C. Hindered rotation of H2 adsorbed interstitially in nanotube bundles. *J. Chem. Phys.* **2002**, *106*, 3371.

(20) Ma, Y. C.; Xia, Y. U.; Zhao, M. W.; Ying, M. J.; Liu, X. D.; Liu, P. J. Collision of hydrogen atom with single walled carbon nanotube: adsorption, insertion and healing. *J. Chem. Phys*. **2001**, *115*, 8152.

(21) Cracknell, R. F. Simulation of hydrogen adsorption in carbon nanotubes. *Mol. Phys.* **2002**, *100*, 2079.

(22) Wang, Q. Y.; Johnson, J. K. Optimization of carbon nanotube arrays for hydrogen adsorption. *J. Phys. Chem. B* **1999**, *103*, 4809.

(23) Wang, Q. Y.; Johnson, J. K. Molecular simulation of hydrogen adsorption in single-walled carbon naotubes and idealized carbon slit pores. *J. Chem. Phys*. **1999**, *110*, 577.

(24) Rzepka, M.; Zlamp, P.; de la Casa-lillo, M. A. Physisorption of hydrogen on microporous carbon and carbon nanotubes. *J. Phys. Chem. B* **1998**, *102*, 10894.

(25) Darkrim, F.; Levesque, D. Monto Carlo simulation of hydrogen adsorption in single-walled carbon nanotubes. *J. Chem. Phys*. **1998**, *109*, 4981.

(26) Darkrim, F.; Levesque, D. High adsorptive property of opened carbon nanotubes at 77 K. *J. Phys. Chem. B* **2000**, *104*, 6773.

(27) Yin, Y. F.; Mays, T.; McEnaney, M. Molecular simulations of hydrogen storage in carbon nanotube arrays. *Langmuir* **2000**, *16*, 10521.

(28) Gu, C.; Gao, G. H.; Yu, Y. X.; Mao, Z. Q. Simulation study of hydrogen storage in single walled carbon nanotubes. *Int. J. Hydrogen Energy* **2001**, *26*, 691.

(29) Williams, K. A.; Eklund, P. C. Monte Carlo simulation of H_2 physisorption in finite-diameter carbon nanotube ropes. *Chem. Phys. Lett*. **2000**, *320*, 352.

(30) Bauschlicher, C. W. High coverage of hydrogen on a (10,0) carbon nanotube. *Nano. Lett.* **2001**, *1*, 223.

(31) Bauschlicher, C. W. Hydrogen and fluorine binding to the sidewall of a (10,0) carbon nanotube. *Chem. Phys. Lett*. **2000**, *322*, 237.

(32) Lee, E. C.; Kim, Y. S.; Jin, Y. G.; Chang, K. J. First principles study of hydrogen adsorption on carbon nanotube surfaces. *Phys. Rev. B* **2002**, *66*, 073415.

(33) Dubot, P.; Cenedese, P. Modeling of molecular hydrogen and lithium adsorption on single walled carbon nanotubes. *Phys. Rev. B* **2001**, *63*, 241402.

(34) Lee, S. M.; Lee, Y. H. Hydrogen storage in single walled carbon nanotubes. *Appl. Phys. Lett*. **2000**, *76*, 2877.

(35) Dresselhaus, M. S.; Williams, K. A.; Eklund, P. C. Hydrogen adsorption in carbon materials. *MRS Bull.* **1999**, *24*, 45.

(36) Cheng, H. M.; Yang, Q. H.; Liu, C. Hydrogen storage in carbon nanotubes. *Carbon* **2001**, *39*, 1447.

(37) Simonyan, V. V.; Johnson, J. K. Hydrogen storage in carbon nanotubes and graphitic nanofibers. *J. Alloys Compd.* **2002**, *330*−*332*, 659.

(38) Darkrim, F. L.; Malbrunot, P.; Tartaglia, G. P. Review of hydrogen storage by adsoption in carbon nanotubes. *Int. J. Hydrogen Energy* **2002**, *27*, 193.

(39) Gordon, P. A.; Saeger, R. Molecular modeling of adsorptive energy storage: Hydrogen storage in single-walled carbon nanotubes. *Ind. Eng. Chem. Res*. **1999**, *38*, 4647.

(40) Zhang, X. R.; Wang, W. C. A density functional study of hydrogen adsorption in single walled carbon nanotube arrays. *Acta Chim. Sin.* **2002**, *60*, 1396.

(41) Johnson, J. K.; Zollweg, J. A.; Gubbins, K. E. The Lennard-Jones equation of state revisited. *Mol. Phys.* **1993**, *78*, 591.

(42) Tjatjopoulos, G. J.; Feke, D. L.; Mann, J. A. Molecule-micropore interaction potentials. *J. Phys. Chem.* **1988**, *92*, 4006.

(43) Tarazona, T. Free-energy density functional for hard spheres. *Phys. Rev. A* **1985**, *31*, 2672; *Phys. Rev. A* **1985**, *32*, 3148.

(44) Tarazona, P.; Marini, B. M. U.; Evans, R. Phase equilibria of fluid interfaces and confined fluids: Nonlocal versus local density functional. *Mol. Phys.* **1987**, *60*, 573.

(45) Weeks, J. D.; Chandler, D.; Anderson, H. C. Role of repulsive forces in determining the equilibria structure of simple liquids. *J. Chem. Phys*. **1971**, *54*, 5237.

(46) Carnahan, N. F.; Starling, K. E. Equation of state for nonattracting rigid spheres. *J. Chem. Phys*. **1969**, *51*, 635.

(47) Lastoskie, C.; Gubbins, K. E.; Quirke, N. Pore size distribution analysis of microporous carbons: A density functional theory approach. *J. Chem. Phys*. **1993**, *97*, 4786.

(48) Ravikovitch, P. I.; Wei, D.; Chueh, W. T.; Haller, G. L.; Neimark, A. V. Evaluation of pore size structure parameters of MCM-41 catalyst supports and catalysts by means of nitrogen and argon adsorption. *J. Phys. Chem. B* **1997**, *101*, 3671.

(49) Alain, E.; Yin, Y. F.; Mays, T.; McEnaney, M. Molecular simulations and measurement of adsorption in porous carbon nanotubes. *Stud. Surf. Catal*. **2000**, *128*, 313.

(50) Simonyan, V. V.; Johnson, J. K.; Kuznetsova, A.; Yates, J. T. Molecular simulation of xenon adsorption on single walled carbon nanotubes. *J. Chem. Phys*. **2001**, *114*, 4180.